Geomechanics and Engineering, *Vol. 28, No. 1 (2022) 89-105*
https://doi.org/10.12989/gae.2022.28.1.089

Distribution of elastoplastic modulus of subgrade reaction for analysis of raft foundations

Kamran Rahgooy[a], Amin Bahmanpour*, Mehdi Derakhshandi[b] and Ahad Bagherzadeh-Khalkhali[c]

Department of Civil Engineering, Science and Research Branch, Islamic Azad University, Tehran, Iran

(Received December 24, 2020, Revised October 5, 2021, Accepted December 1, 2021)

Abstract. The behavior of the soil subgrade is complex and irregular against loads. When modeling, the soil is often replaced by a more straightforward system called a subgrade model. The Winkler method of linear elastic springs is a popular method of soil modeling in which the spring constant shows the modulus of subgrade reaction. In this research, the factors affecting the distribution of the modulus of subgrade reaction of elastoplastic subgrades are examined. For this purpose, critical theories about the modulus of subgrade reaction were examined. A square raft foundation on a sandy soil subgrade with was analyzed at different internal friction angles and Young's modulus values using ABAQUS software. To accurately model the actual soil behavior, the elastic, perfectly plastic constitutive model was applied to investigate a foundation on discrete springs. In order to increase the accuracy of soil modeling, equations have been proposed for the distribution of the subgrade reaction modulus. The constitutive model of the springs is elastic, perfectly plastic. It was observed that the modulus of subgrade reaction under an elastic load decreased when moving from the corner to the center of the foundation. For the ultimate load, the modulus of subgrade reaction increased as it moved from the corner to the center of the foundation.

Keywords: elastic; finite element method; modulus of subgrade reaction; perfectly plastic spring; raft foundation

1. Introduction

A raft foundation is a type of shallow foundation that is usually used for buildings located on soft soil or that should transfer large loads to the ground. Essentially, a raft foundation is a rigid slab that acts as a single member that tolerates the column load and transfers it to the ground over the entire surface of the structure. The load-bearing capacity and settlement must be controlled when designing a raft foundation. Study of the effects of the interaction between the soil and structure is of special importance, particularly for the modulus of subgrade reaction. This parameter is dependent on the geometric specifications of the foundation and the mechanical properties of the soil.

Several methods have been proposed to obtain the modulus of subgrade reaction, including numerical methods such as the Winkler method. The design of structures with raft foundations is often performed by static analysis of concrete foundations on Winkler springs. When Winkler's method (1867) for obtaining the modulus of subgrade reaction has been simplified, it has been proven that incorrect results are obtained. This effect is due to the lack of bending moments in the raft foundations, shear stresses in the soil, the independence of the Winkler springs and the failure to consider settlement around the foundation soil (Bowles 1997).

The first and simplest model for investigating soil-foundation interaction is the model proposed by Winkler (1867). In this model, the deformation of a point of the soil subgrade is assumed to be proportional to the amount of stress at that point and the effect of stress on and displacement of the other points is ignored. Hertz (1884) first used this model to study the soil-foundation interaction. Zimmerman (1888) used this model to study the stress and settlement on railway tracks. This model has been widely used for the analysis of beams and plates on elastic subgrades, especially by Hayashi (1921) and Vlasov and Leontiev (1966). Terzaghi (1955) provided a method for estimating spring constants when determined the modulus of subgrade reaction.

Most research on determination of the horizontal and vertical modulus of subgrade reaction was done by Terzaghi (1955). Among the factors examined by Terzaghi (1955), were the foundation dimensions, the shape of the foundation and its depth. Terzaghi used a plate loading test on the ground using a plate with a 1-inch diameter and these results were extended to other foundation widths. It has been suggested that the approximate horizontal and vertical modulus of subgrade reactions in different soils should be determined.

Other researchers who have examined the plate loading test for determination of the modulus of subgrade reaction include Miner and Seaston (1955), Bond (1961), Teng (1962), Broms (1964), Bowles (1997), Beri (1987), Arnolds (1980), Al Sand (1933) and Ismael (1985, 1996). Kome *et*

*Corresponding author, Assistant Professor
E-mail: Aminbahmanpour@srbiau.ac.ir
[a]Ph.D. Student
E-mail: Kamran.Rahgooy@srbiau.ac.ir
[b]Assistant Professor
E-mail: M-Derakhshandi@srbiau.ac.ir
[c]Assistant Professor
E-mail: A-Bagherzadeh@srbiau.ac.ir

ISSN: 2005-307X (Print), 2092-6219 (Online)

al. (2008) calculated the transverse deformation of foundations using the Winkler model. Ziaee Moayed (2012) calculated the transverse deformation of the foundations using the Winkler (1867) model. These studies included examination of the effect of the foundation dimensions, soil layers and soil stress and strain on the modulus of subgrade reaction. Each of the many researchers who have investigated this parameter have studied the factor in different soil types with different loadings. These include Holtz (1991), Worku (2009), Dey *et al*. (2011), Garg and Hora (2012), Abdoulaye Shall *et al*. (2013), Naeini *et al*. (2014), Basil (2015), Lee *et al*. (2015), Jeong *et al*. (2017), Figueira *et al*. (2018), Jamil and Ahmad (2019), and Teli *et al*. (2020). The effect of the variations in the modulus of subgrade reaction in the inelastic load range in rigid piles under lateral load has been analyzed by Qin and Dong Guo (2014). Meanwhile, some other studies have used optimization methods for the similar application but related to renewable energy advancement (Amini *et al.* 2020, Amini *et al.* 2021).

Because of the simplifications introduced in these theories, the behavior displayed by the soil is, in most cases, not the same as the actual behavior of the soil and there were some approximations. The approximations can cause errors in the calculation of the modulus of subgrade reaction at times. It should be noted that, when using a simplified model, the results should be acceptable and the approximation should not cause significant error. The relationships introduced by Biot (1937), Reti (1967), and Bowles (1997) assume that the modulus of subgrade reaction across the foundation is the same.

The present research investigated the factors affecting the modulus of subgrade reaction in the design and analysis of foundations. The finite element method has been used for numerical modeling. This research investigates the effect of factors such as the modulus of elasticity and friction angle of sandy soil on the modulus of subgrade reaction. The distribution of the modulus of subgrade reaction in the longitudinal direction of the raft foundation under the ultimate load, half-ultimate load and elastic load have been examined. As a result, a raft foundation is proposed that has been modeled on springs with an elastic, perfectly plastic constitutive model.

2. Methodology

In this study, 3D finite element (FE) analysis has been used to establish accurate estimates of the raft deflections. The analysis was performed using the FE software ABAQUS. The computational model consisted of a block of 8-node first-order hexahedral elements (C3D8) representing the soil and foundation.

The Mohr-Coulomb constitutive model was used for convergence and a small cohesion value of 1 KPa has been assumed for the soil. Internal friction angles of 35°, 37°, and 39° were considered. This small range for the internal friction angle has been used because of the considerable effect of shear strength, bearing capacity and ultimate load distribution from the soil friction angle under a sandy soil foundation. The modulus of elasticity of the sandy soil was selected to be 50, 80, and 123 MPa. The elasticity and plasticity specifications of the sandy soil are given in Table 1.

Table 1 Material specifications of soil

Model	Poisson's ratio μ_s	Modulus of elasticity (MPa) E_s	Internal friction angle φ
A-1	0.3	123	39
B-1	0.3	80	39
C-1	0.3	50	39
A-2	0.3	123	37
B-2	0.3	80	37
C-2	0.3	50	37
A-3	0.3	123	35
B-3	0.3	80	35
C-3	0.3	80	35

Table 2 Material specifications (Loukidis and Tamiolakis 2017)

Material	Value
E_s(MPa)	10
E_c(GPa)	32
μ_s	0.3
μ_c	0.2
γ (kN/m^3)	17.62
γ_c(kN/m^3)	24

The concrete foundation had a modulus of elasticity (E_c) of 2.1 GPa and a Poisson's ratio (μ_c) of 0.2. The soil had a modulus of elasticity (E_s) of 10 MPa and a Poisson's ratio (μ_s) of 0.3. The specific weight of concrete (γ_c) in the foundation and soil (γ) were 24 and 18.1 kN/m^3, respectively. Table 1 shows the specifications of the materials used. A raft foundation with dimensions of 10×10×0.5 m has also been considered in the modeling.

The soil was modeled as an isotropic continuum with yielding that is described by the Mohr-Coulomb yield criterion as

$$\tau = c + \sigma_n \tan\varphi \quad (1)$$

In Eq. (1), c is the cohesion of the soil, σ_n is the normal vertical stress, φ is the internal friction angle and, τ is the shear stress.

For verification, the results of FE analysis by Loukidis and Tamiolakis (2017) have been used. In their research, a concrete slab with dimensions of 10×10×0.5 m was placed on an elastic subgrade with sandy soil having the specifications listed Table 2. Concentrated loads then were positioned at the edges and the center of the slab, as shown in Fig. 1.

After loading in ABAQUS, the amount of settlement under the foundation is measured from the edge to the center. Then these results are compared with the results obtained in the modeling of Loukidis and Tamiolakis

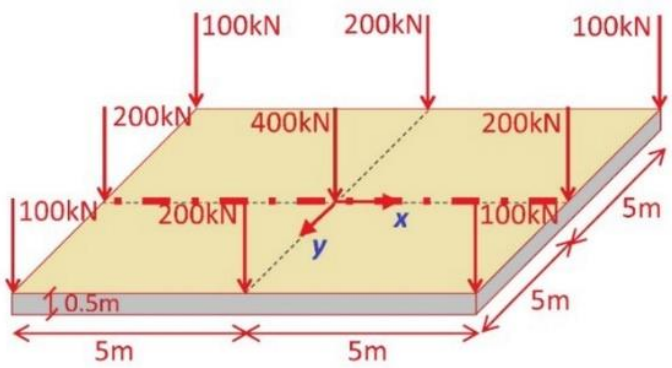

Fig. 1 Load applied to foundation and dimensions of concrete slab (Loukidis and Tamiolakis 2017)

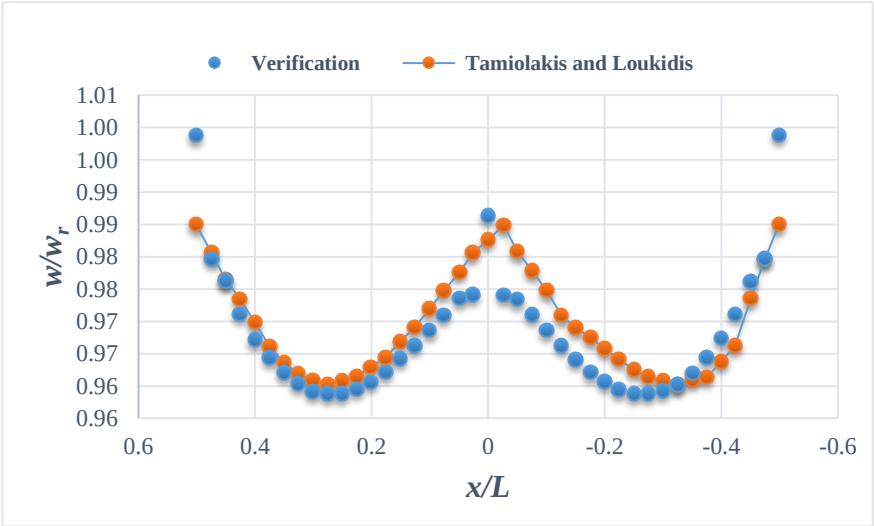

Fig. 2 Relative settlement between current model and Loukidis and Tamiolakis (2017)

(2017). Fig. 2 compares the relative settlement from the present research and that of Loukidis and Tamiolakis (2017). The relative settlement (w/w_r) error in the direction of the foundation length at the center and edge of the foundation was 0.09% and 1.1%, respectively, which is acceptable.

3. Results

The effect of the modulus of elasticity and internal friction angle of the soil on the distribution of the modulus of subgrade reaction and its effect on the stiffness of elastoplastic springs were investigated and the results are presented in this section. In the elastic load, the half-ultimate load, and the ultimate load, the distribution of the modulus of subgrade reaction were investigated.

In this study, a uniform distributed load is applied to the raft foundations in ABAQUS software. The intensity of the uniform distributed load increases from zero to the ultimate limit state.

3.1 Distribution modulus of subgrade reaction in elastic range in sandy soil

Fig. 3 shows the 2D and 3D distributions of the relative modulus of subgrade reaction in the elastic range for modulus of elasticity values of 50, 80, and 123 MPa.

It was observed that, by moving from the corner to the center of the slab in the elastic range, the modulus of subgrade reaction of the foundation decreased. This means that, in the elastic range, the modulus of subgrade reaction at the corners of the foundation has been maximized. Overall, the value of the relative modulus of subgrade reaction decreased by 12.3% with a decrease in the modulus of elasticity from 123 to 50 MPa.

In the elastic range, with an increase in the modulus of soil elasticity, the modulus of subgrade reaction decreased when moving from the corner to the center of the slab. For example, for a modulus of elasticity of 123 MPa, the rate of reduction of the modulus of subgrade reaction was 33%. With a reduction in the modulus of elasticity to 50 MPa, the modulus of subgrade reaction decreased by 50%.

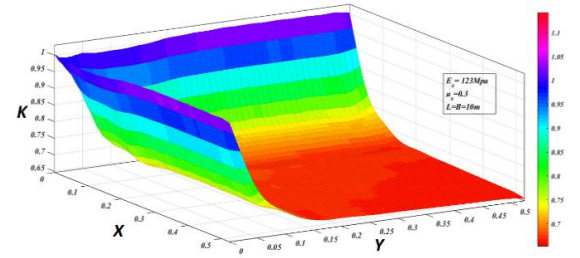

(a1) 3D Distribution (E_s = 123 MPa)

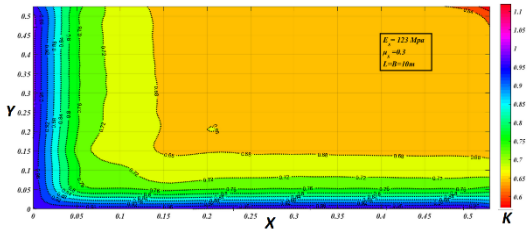

(a2) 2D Distribution (E_s = 123 MPa)

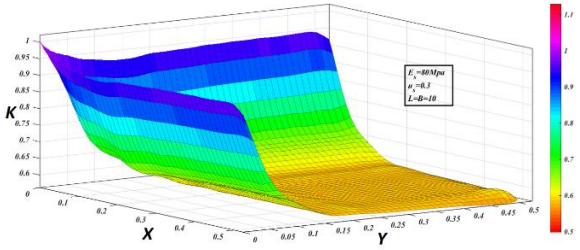

(b1) 3D Distribution (E_s = 80 MPa)

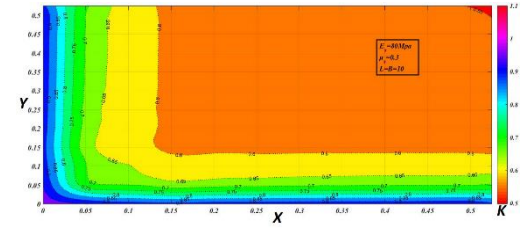

(b2) 2D Distribution (E_s = 80 MPa)

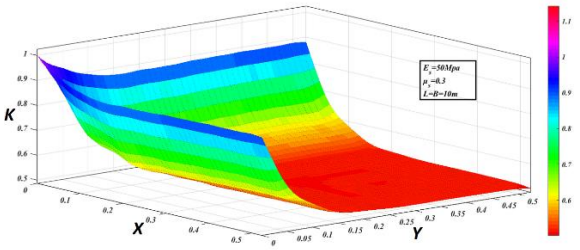

(c1) 3D Distribution (E_s = 50 MPa)

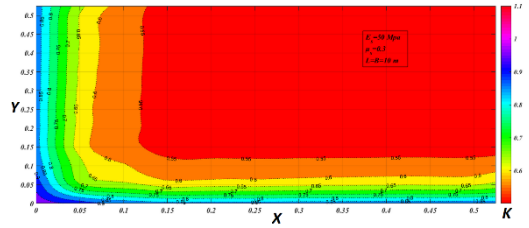

(c2) 2D Distribution (E_s = 50 MPa)

Fig. 3 Distribution of relative modulus of subgrade reaction for Elastic laod

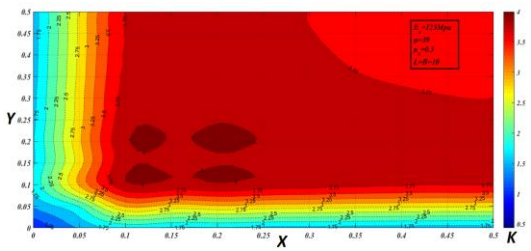

(a) φ = 39°

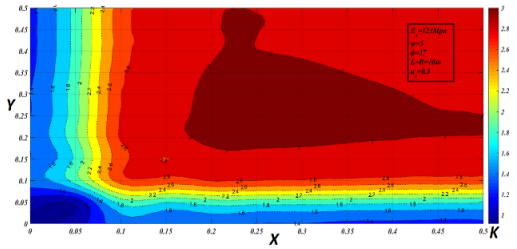

(b) φ = 37°

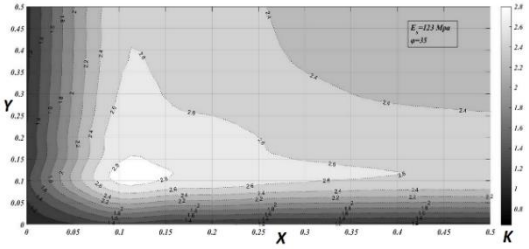

(c) φ = 35°

Fig. 4 Distribution of relative modulus of subgrade reaction for half-ultimate load at E_s = 123 MPa

3.2 Distribution of modulus of subgrade reaction for the half-ultimate load

The sandy soil was examined at modulus of elasticity values of 123, 80 and 50 MPa and internal friction angles of 35°, 37° and 39° using two forms of continuum FE as well as vertical elastic, perfectly plastic discrete springs instead of the casing soil. Figs. 4 to 6 show the 2D polynomials of the modulus of subgrade reaction for the half-ultimate load at friction angles of 35° to 39° and modulus of elasticity

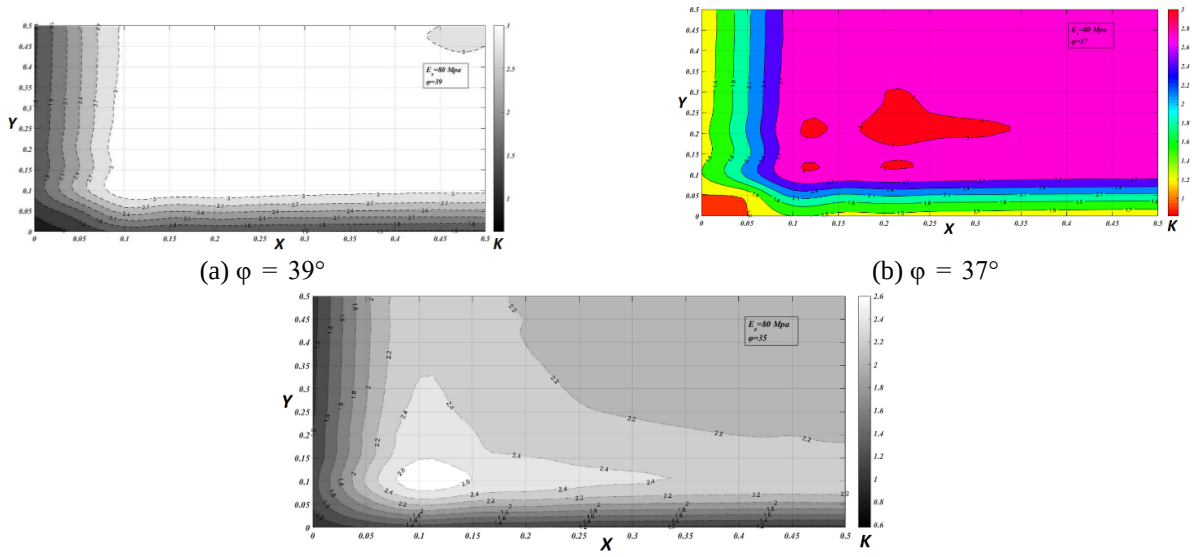

(a) φ = 39° (b) φ = 37°

(c) φ = 35°

Fig. 5 Distribution of relative modulus of subgrade reaction for half-ultimate load at E_s = 80 MPa

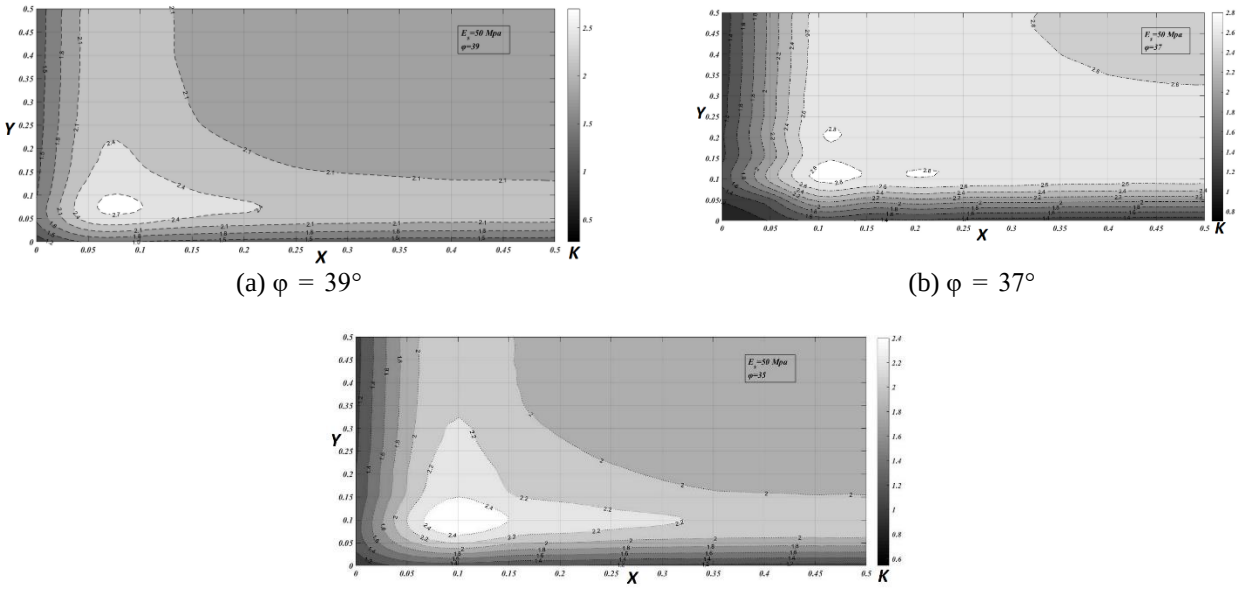

(a) φ = 39° (b) φ = 37°

(c) φ = 35°

Fig. 6 Distribution of the relative modulus of subgrade reaction for half-ultimate load at E_s = 80 MPa

values of 50 to 123 MPa for a raft foundation in sandy soil.

For the half-ultimate load, the modulus of subgrade reaction increased as it moved from the corner of the slab to the center. This means that, for the half-ultimate load, the modulus of subgrade reaction at the corners of the foundation were minimized. When moving from the corner to the center of the slab, the modulus of subgrade reaction for a modulus of elasticity of 123 MPa and friction angle of 35° increased 2.7- to 3-fold.

3.3 Distribution of modulus of subgrade reaction for ultimate load

Sandy soil with a modulus of elasticity of 50, 80 and 123 MPa, internal friction angles of 35°, 37°, and 39° for two forms of continuum FE and vertical elastic, perfectly plastic discrete springs instead of casing soil was examined. The 2D and 3D polynomials of the modulus of subgrade reaction for the ultimate load at friction angles of 35° to 39° and modulus of elasticity values of 50 to 123 MPa for raft foundations in sandy soil are shown in Figs. 7-9.

The modulus of elasticity was held constant at this stage and the friction angle was varied from 35° to 39°. The settlement and load were verified for the ultimate load. The curves show that, for the ultimate load, as the modulus of subgrade reaction moved from the corner of the foundation

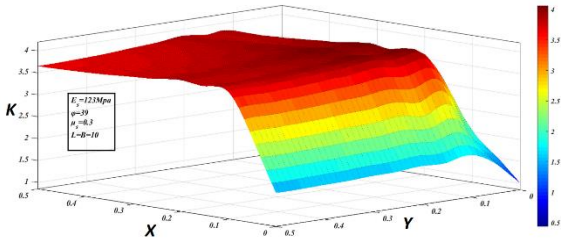

(a1) 3D Distribution (φ = 39°)

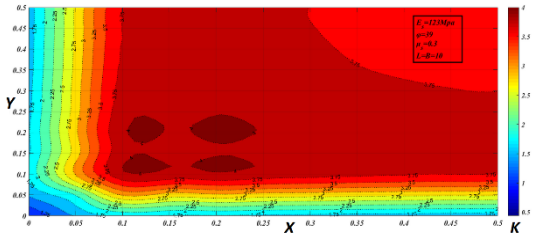

(a2) 2D Distribution (φ = 39°)

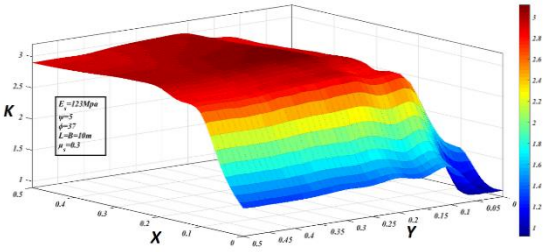

(b1) 3D Distribution (φ = 37°)

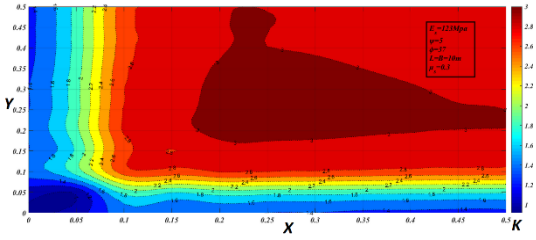

(b2) 2D Distribution (φ = 37°)

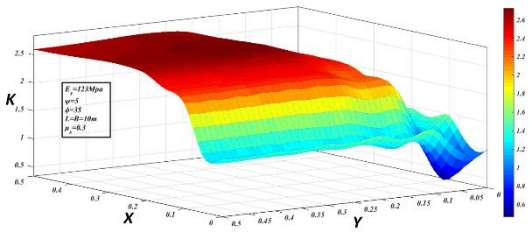

(c1) 3D Distribution (φ = 35°)

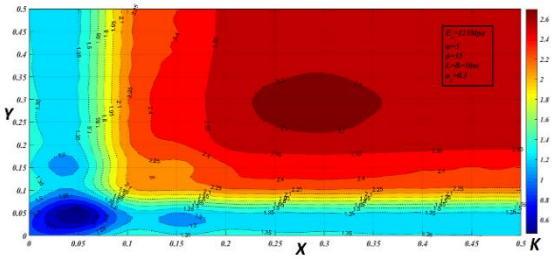

(c2) 2D Distribution (φ = 35°)

Fig. 7 Distribution of the relative modulus of subgrade reaction for the ultimate load at E_s = 123 MPa

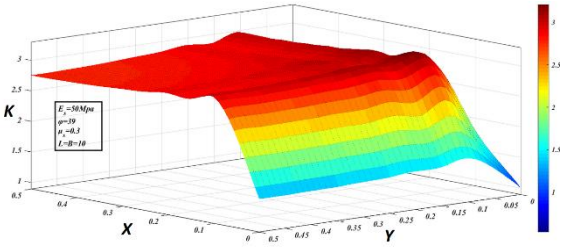

(a1) 3D Distribution (φ = 39°)

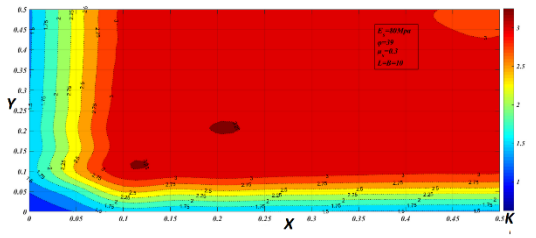

(a2) 2D Distribution (φ = 39°)

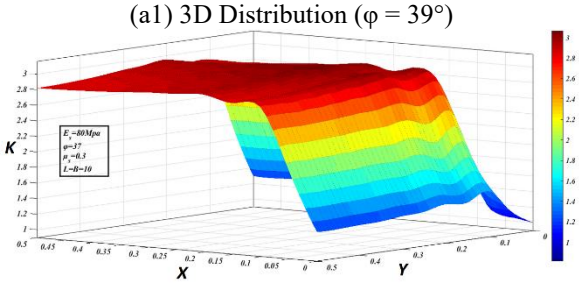

(b1) 3D Distribution (φ = 37°)

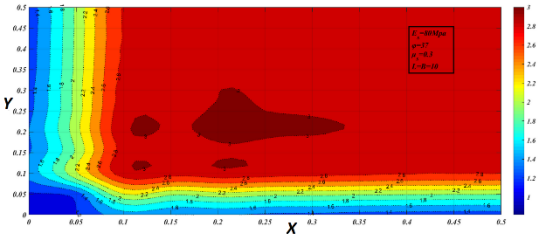

(b2) 2D Distribution (φ = 37°)

Fig. 8 Distribution of the relative modulus of subgrade reaction for the ultimate load at E_s = 80 MPa

to the center, it increased 2.4 to 3.25 times. As it moved from the corner to the center of the slab, the modulus of subgrade reaction for a modulus of elasticity of 123 MPa and friction angle of 35° increased 3-fold. It can be said that, in the plastic range (ultimate load), the modulus of subgrade reaction at the corners of the foundation were minimized.

Reducing the friction angle from 39° to 35° at a constant

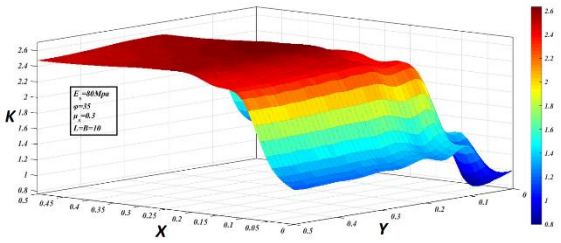

(c1) 3D Distribution (φ = 35°)

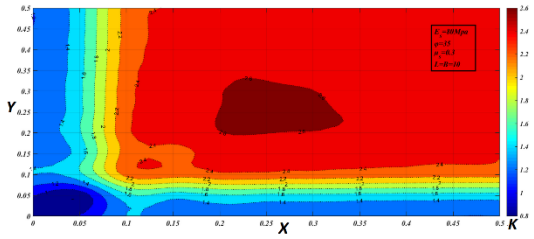

(c2) 2D Distribution (φ = 35°)

Fig. 8 Continued-

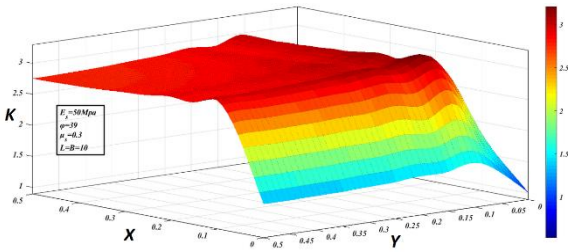

(a1) 3D Distribution (φ = 39°)

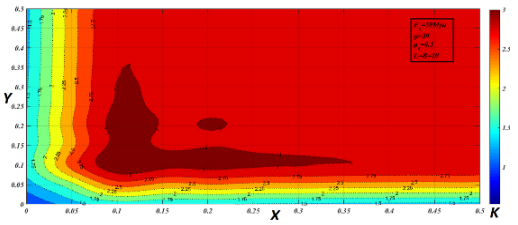

(a2) 2D Distribution (φ = 39°)

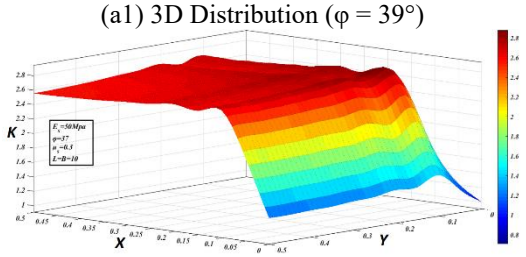

(b1) 3D Distribution (φ = 37°)

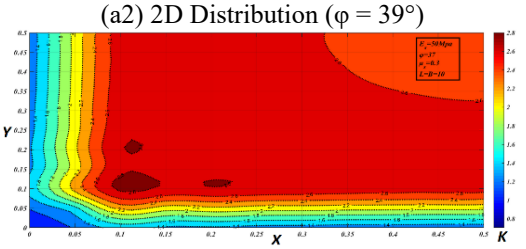

(b2) 2D Distribution (φ = 37°)

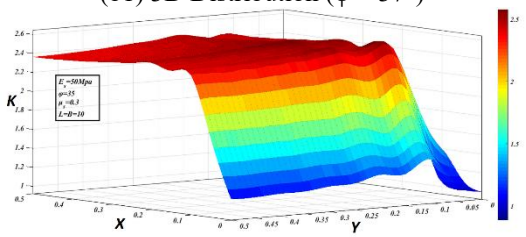

(c1) 3D Distribution (φ = 35°)

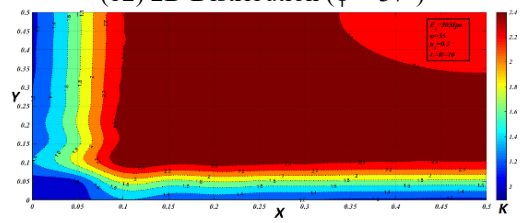

(c2) 2D Distribution (φ = 35°)

Fig. 9 Distribution of the relative modulus of subgrade reaction for the ultimate load at E_s = 50 MPa

modulus of elasticity reduced the modulus of subgrade reaction by 30%. This occurred because the stress distribution under the foundation in the soil was not uniform and the final stress at the corners of the foundation was less than the final stress at the center. At the center of the foundation, the confining stress was greater than the confining stress at the corners and edges of the foundation because shear failure requires less vertical stress at the corners (Rajashekhar *et al*. 2011). This reduced the modulus of subgrade reaction in the plastic range at the corners and edges of the foundation.

3.4 Results of stress-displacement curve

Figs. 10(a)-10(c) shows the stress-displacement curvesat the center of the foundation for modulus of elasticity values of 50, 80, and 123 MPa and internal friction angles of 35°, 37° and 39°.

Figs. 10(a)-10(c) shows that, at a single modulus of elasticity and constant settlement, the final stress increased as the internal friction angle increased. When the modulus of elasticity increased and the friction angle and settlement were held constant, the vertical stress increased. An increase in the modulus of elasticity from 50 to 123 MPa increased the final stress by 50%. This demonstrates that the effect of the modulus of elasticity is significant when calculating the final stress. The time-history curve for vertical stress is shown in Fig. 11 for the corner and center of the foundation at modulus of elasticity values of 50 and 80 MPa at an internal friction angle of 35°.

As shown in Fig. 11, the amount of stress at the foundation corners at the final moment (ultimate load) was less than the amount of stress at the center of the foundation. It was observed that the amount of vertical stress in the center of the foundation was about 2.3 times greater than the stress at the corner. Fig. 12 shows the results for final displacement of the foundation (u_p).

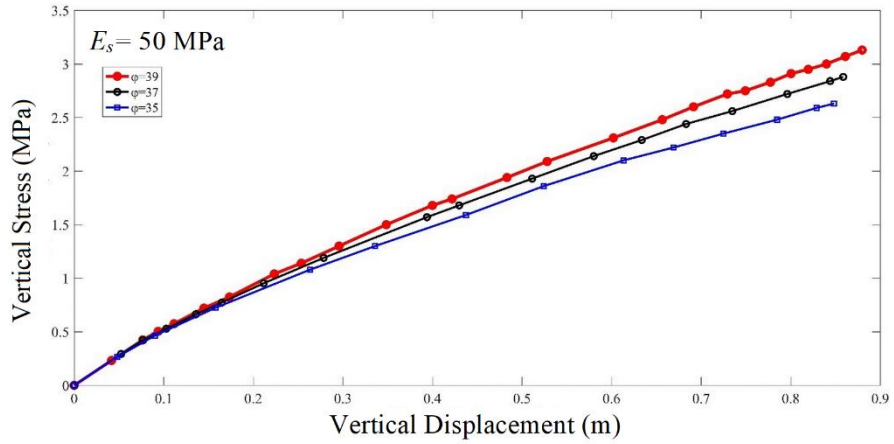

(a) E_s =50 MPa

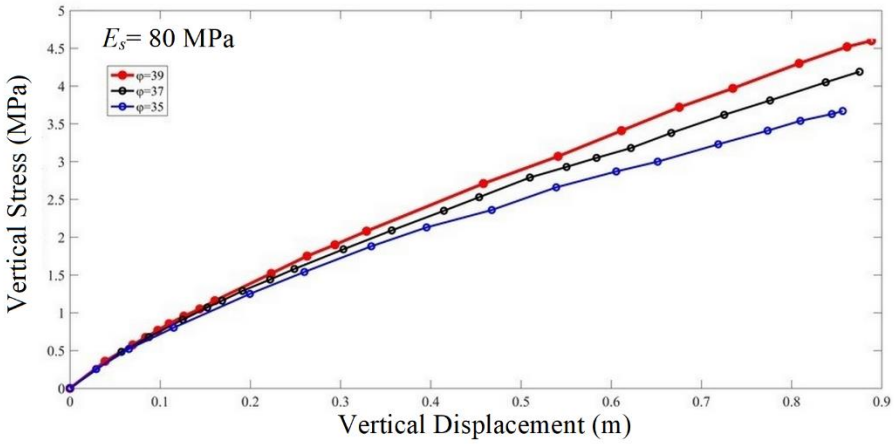

(b) E_s =80 MPa

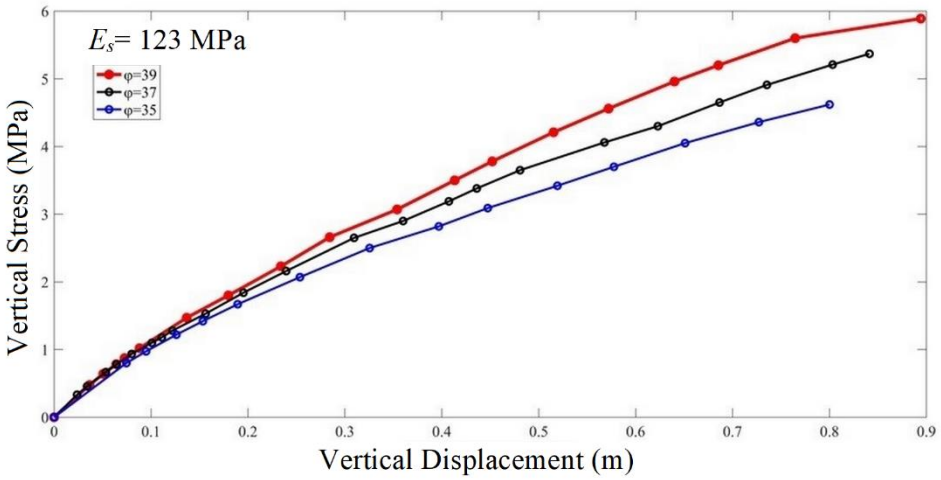

(c) E_s =123 MPa

Fig. 10 Vertical stress-vertical displacement curve according to friction angle

3.5 Mass-spring modeling results vs. continuum finite element analysis (cFEA) model

The forces created in the springs were investigated and the results were used to model the load-settlement curve in a cFEA in the mass-spring modelling stage for the elastic, perfectly plastic condition. This stage of modeling was done after the initial analysis. Back calculations is used for mass-springs modelling to obtain a elastoplastic model for springs (load-displacement).

The linear springs and elastoplastic springs do not stretch at any point because the tensile strength of sandy

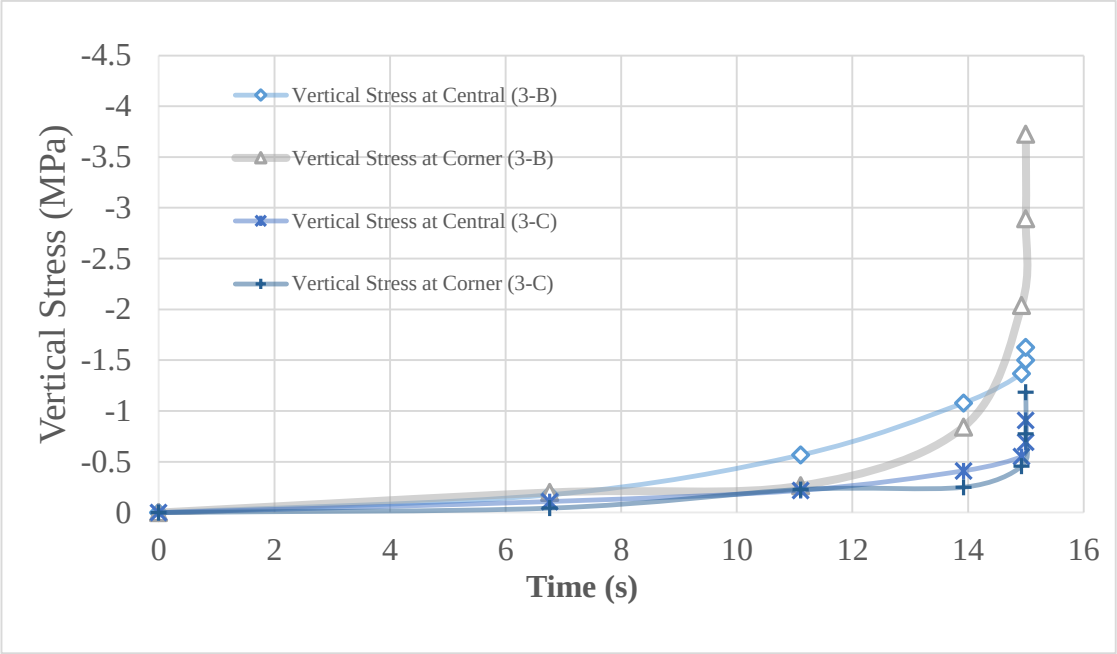

Fig. 11 Time-history curve of vertical stress at the corner and center of the slab for an internal friction angle of 35° and modulus of elasticity values of 50 and 80 MPa

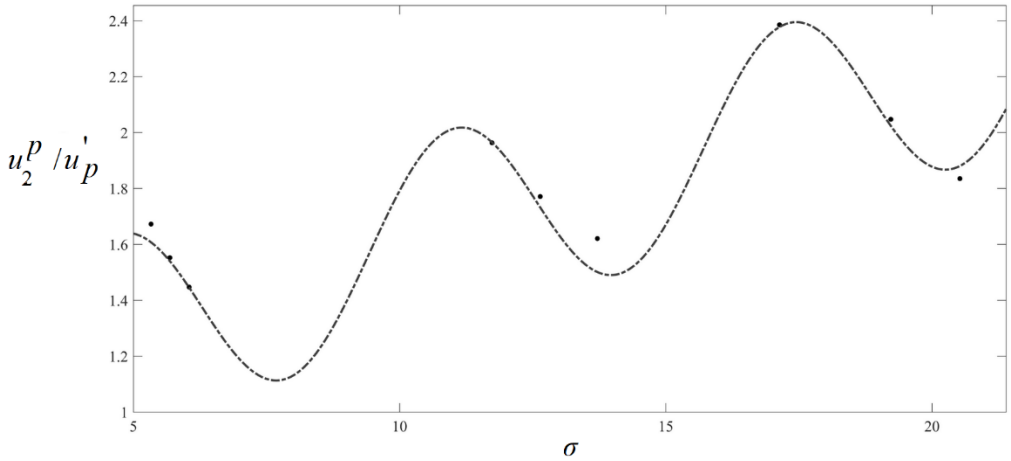

Fig. 12 Final displacement curve for ultimate stress

soil is very low; therefore, in the initial analysis, the stretched springs were identified and then removed from the model and it then was reanalyzed. This stage continued until none of the springs had stretched. The ultimate stress and final settlement of the springs are presented in Figs. 13 and 14. In Fig. 13, the average error obtained was 0.7%, which is acceptable. It could be observed that the vertical stress increased when moving from the corner to the center of the foundation.

Figs. 13 and 14 show that the results of both the cFEA and mass-spring (SP) models were very similar, such that the displacement error between the discrete spring model and the cFEA model was 5.6%. In general, it can be stated that moving from the edge to the center of the foundation decreased the displacement. It can be said that, when the springs are modeled, settlement at the foundation corners is less than at the center after the application of an extensive load. This occurs because the stiffness of the springs at the corners in the plastic range is less than that of the springs at the center.

3.6 Proposed equations for modulus of subgrade reaction distribution

The spatial distribution of the relative modulus of subgrade reaction in the elastic range is a six-degree symmetric polynomial (Fig. 3). The coefficients of Eq. (5) are listed in Table 3. c_0, c_1, c_2, b_1 and b_2 are the coefficients of Eq. (5). In Eq. (2), coefficient K_e is the relative modulus of subgrade reaction in the elastic load range. This is the ratio of the modulus of subgrade reaction at the desired point on the raft foundation, K_{s_e}, to the modulus of subgrade reaction at the corner of the foundation, $K_{s_{ce}}$.

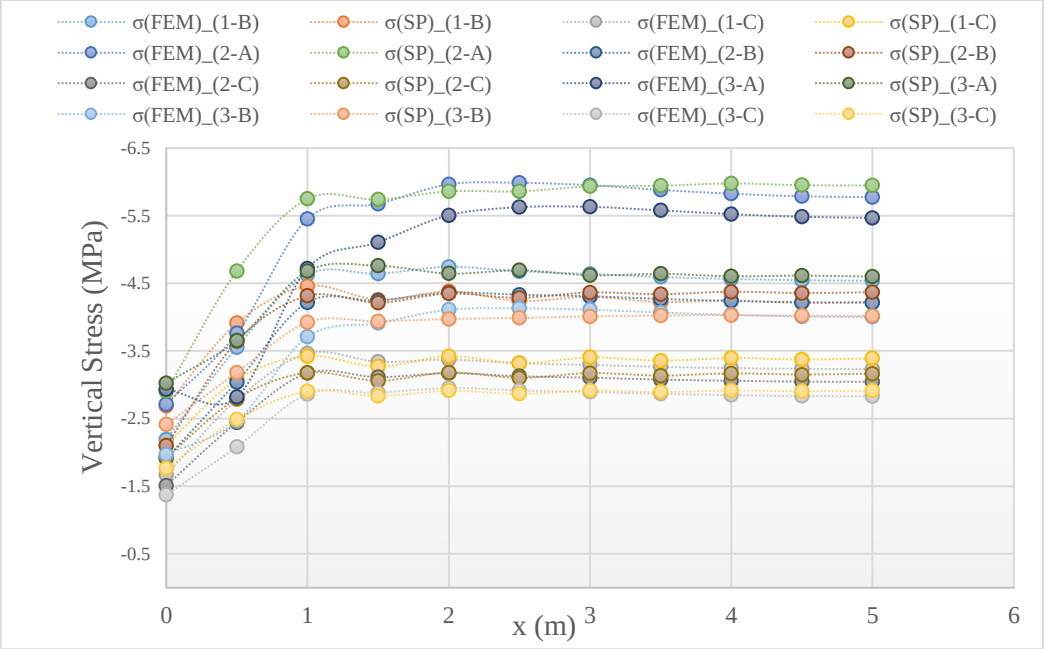

Fig. 13 ultimate vertical stress along the central axis of the foundation

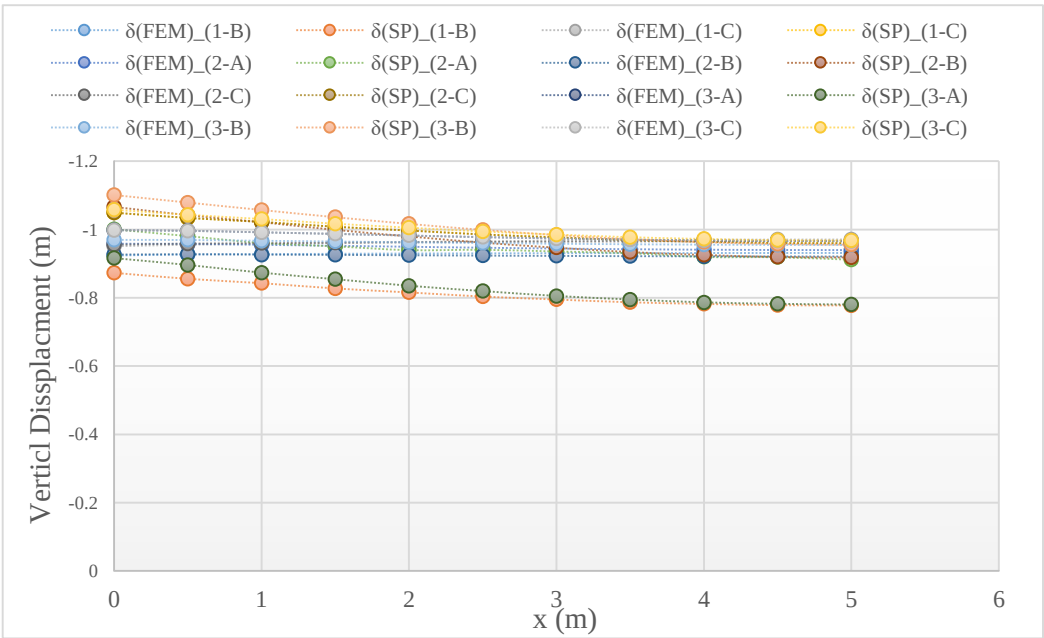

Fig. 14 Final vertical displacement along the central axis of the foundation

$$K_e = \frac{K_{s_e}}{K_{s_{c_e}}} \tag{2}$$

In Eq. (3), coefficient X is the relative length of the raft foundation, in which x is the length of the desired point from the origin of the coordinate, assuming that this origin is at the corner of the foundation and B is the width of the foundation.

$$X = \frac{x}{B} \tag{3}$$

In Eq. (4), coefficient Y is the relative width of the raft foundation, y is the width of the desired point from the origin of the coordinate assuming that this origin is at the corner of the foundation and L is the length of the foundation.

$$Y = \frac{y}{L} \tag{4}$$

In Eq. (6), H is the height of the bottom layer of the foundation in terms of unit length and A is the area of the foundation in terms of square units of length. The factors s_{H_1} and s_{H_2} introduce the influence of the presence of an undeformable substratum at depth H below the raft foundation and the area of the foundation A. The factors s_x and s_y introduce the influence of the length (x) and

Table 3 Coefficients for Eq. (5)

E_s(MPa)	c_0	c_1	c_2	b_1	b_2
123	0.67	2.6	2.6	-0.8121	-0.812
80	0.58	2.7	2.7	-0.84	-0.84
50	0.508	2.72	2.72	-0.8446	-0.8446

Table 4 Coefficients for Eq. (8)

Coef	A-1	B-1	C-1	A-2	B-2	C-2	A-3	B-3	C-3
c_0'	3.835	3.078	2.553	2.977	2.781	2.644	2.614	2.446	2.323
c_1'	1.322	2.584	3.464	1.842	2.24	2.633	2.947	3.331	3.373
c_2'	1.322	2.584	3.464	1.842	2.24	2.633	2.947	3.331	3.373
b_1'	−1.05	−1.05	−1.05	−1.0542	−1.037	−1.025	−1.033	−1.018	−1.004
b_2'	−1.05	−1.05	−1.05	−1.0542	−1.037	−1.025	−1.033	−1.018	−1.004
a	−9.207	−9.207	28.86	−1.004	−15.52	−7.164	−1.551	7.404	−15.4
b	−1.004	−1.462	−8.949	−1.004	−3.373	−1.028	1.267	3.416	5.479

Table 5 Coefficients for Eq. (10)

Coef	*A-1*	*B-1*	*C-1*	*A-2*	*B-2*	*C-2*	*A-3*	*B-3*	*C-3*
c''_0	3.82	3.1	2.885	3	2.92	2.65	2.7	2.543	2.443
c''_1	2.622	2.73	3.47	1.75	2.24	2.745	1.123	1.55	2.212
c''_2	2.622	2.73	3.47	1.75	2.24	2.745	1.123	1.55	2.212
b''_1	−1.09	−1.052	−1.035	−1.05	−1.048	−1.026	−1.028	−1.023	−1.016
b''_2	−1.09	−1.052	−1.035	−1.05	−1.048	−1.026	−1.028	−1.023	−1.016

width (y) of the desired point from the origin of the coordinate.

$$K_e = F(X,Y) = c_0 + (c_1X + b_1)^6 + (c_2Y + b_2)^6 \tag{5}$$

$$\begin{cases} s_x = \left[\left(\frac{H}{B}\right)^{0.51}\left(\frac{x}{B}\right) - 1\right]^6 \quad 0 \le x \le \frac{B}{2} & (a) \\ s_y = \left[\left(\frac{H}{L}\right)^{0.51}\left(\frac{y}{L}\right) - 1\right]^6 \quad 0 \le y \le \frac{L}{2} & (b) \\ s_{H_1} = 0.47 \exp\left(\left(\frac{A}{H^2}\right)^2 E_s\right) & (c) \\ s_{H_2} = \left(\frac{A}{H^2}\right)^2 \left(1 + \left(\frac{H^2}{A}\right)^{0.4}\right) & (d) \end{cases} \tag{6}$$

Finally, by combining Eqs. (6(a))-(6(d)) in Eq. (5), Eq. (6(e)) was obtained

$$K_{s_e} = s_{H_1} K_{s_{c_e}} \left[1 + s_{H_2}(s_x + s_y)\right] \tag{6e}$$

The spatial distribution of the relative modulus of subgrade reaction for the half-ultimate load is an eight-degree polynomial (Figs. 4-6). The coefficients for this polynomial (Eq. (8(a))) are listed in Table 4. c'_0, c'_1, c'_2, b'_1,b'_2, a and, b is the coefficients in Eq. (8). In Eqs. (7) and (8(a)), coefficient K_h is the relative modulus of subgrade reaction for the half-ultimate load, which is the ratio of the modulus of subgrade reaction for the half-ultimate load at the desired point of the raft foundation, K_{s_h}, to the modulus of subgrade reaction for the half-ultimate load at the corner of the raft foundation, $K_{s_{c_h}}$.

$$K_h = \frac{K_{s_h}}{K_{s_{c_h}}} \tag{7}$$

$$\begin{cases} K_h = H(X,Y) = M(X,Y) + N(X,Y) & (a) \\ M(X,Y) = c_0' - (c_1'X + b_1')^8 - (c_2'Y + b_2')^8 & (b) \\ N(X,Y) = aXY\left(XY - \frac{b}{a}\right) & (c) \end{cases} \tag{8}$$

The spatial distribution of the relative modulus of subgrade reaction for the ultimate load is an eight-degree polynomial (Figs. 7-9).

The coefficients of this polynomial (Eq. (10)) are listed in Table 5. c''_0, c''_1, c''_2, b''_1 and, b''_2 is the coefficients in Eq. (8). In Eqs. (9) and (10), coefficient K_p is the relative modulus of subgrade reaction for the ultimate load, which is the ratio of the modulus of subgrade reaction for the ultimate load at the desired point on the raft foundation, K_{s_p}, to the modulus of subgrade reaction for the half-ultimate load at the corner of the raft foundation, $K_{s_{c_p}}$.

In Eq. (11), H is the height of the bottom layer of the foundation in terms of unit length and A is the area of the foundation in terms of square units of length.

$$K_p = \frac{K_{s_p}}{K_{s_{c_p}}} \tag{9}$$

$$G(X,Y) = c_0'' - (c_1''X + b_1'')^8 - (c_2''Y + b_1'')^8 \tag{10}$$

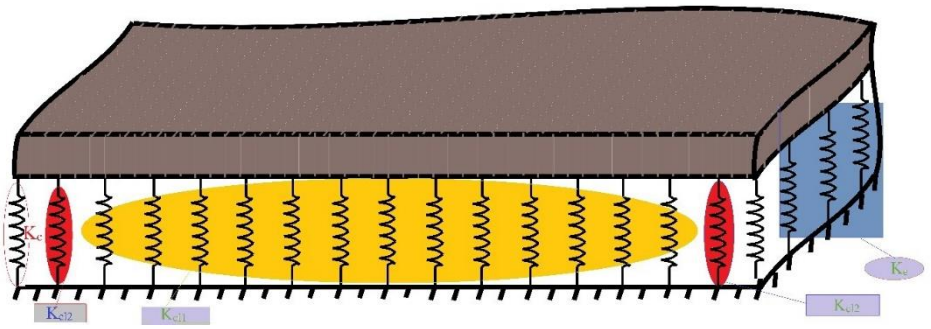

(a) vertical spring distribution and schematic zoning of vertical springs

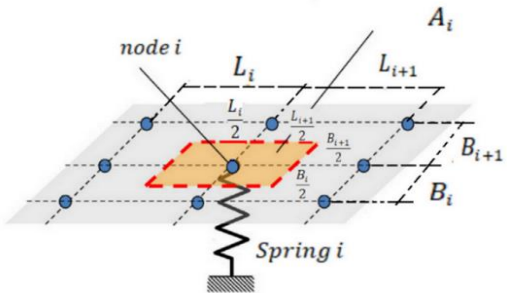

(b) spring load-bearing surface (Loukidis and Tamiolakis 2017)

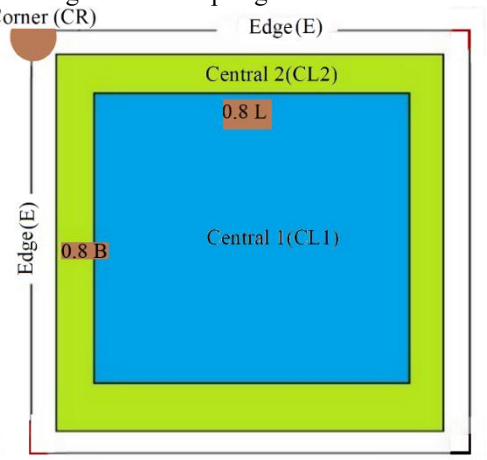

(c) division of raft into zones having different modulus of subgrade reaction values

Fig. 14 Soil modeling with springs

$$
\begin{aligned}
c''_1 &= \left(\frac{H}{B}\right)^{1.33} + \left[\left(\frac{H}{B}\right)^{-0.18}\tan(\varphi) - \left(\frac{H}{B}\right)^{0.19}\right]\ln(E_s) \quad (a)\\
c''_2 &= \left(\frac{H}{L}\right)^{1.33} + \left[\left(\frac{H}{L}\right)^{-0.18}\tan(\varphi) - \left(\frac{H}{L}\right)^{0.19}\right]\ln(E_s) \quad (b)\\
b''_1 &= -\left[\left(\frac{H}{B}\right)^{0.366} + \left(\left(\frac{H}{B}\right)^{-1.733}\tan(\varphi) + \left(\frac{H}{B}\right)^{-1.705}\right)\ln(E_s)\right] \quad (c)\\
b''_2 &= -\left[\left(\frac{H}{L}\right)^{0.366} + \left(\left(\frac{H}{L}\right)^{-1.733}\tan(\varphi) + \left(\frac{H}{L}\right)^{-1.705}\right)\ln(E_s)\right] \quad (d)\\
c''_0 &= \left(\frac{H^2}{A}\right)^{0.436} + \left[\left(\frac{H^2}{A}\right)^{-0.224}\tan(\varphi) + \left(\frac{H^2}{A}\right)^{-0.261}\right]\ln(E_s) \quad (e)
\end{aligned}
\tag{11}
$$

3.7 Soil modeling with spring

To model the soil with springs, and for more accurate modeling of the soil, vertical springs were used with the elastic, perfectly plastic constitutive model. For the horizontal springs, elastic Winkler springs having a constant stiffness were used. The load-bearing surface of each spring can be obtained according to the distance between the springs (Loukidis and Tamiolakis 2017). The load-bearing area of spring i, denoted by A_i, is shown in Fig. 14(b). Eq. (12) has been is used to calculate A_i as

$$A_i = \frac{1}{4}(B_{i+1} + B_i)(L_{i+1} + L_i) \tag{12}$$

The stiffness of each spring, K_{sp_i} can be calculated using the modulus of subgrade reaction as

$$K_{sp_i} = K_s \times A_i \tag{13}$$

When modeling these foundations, the horizontal distance between the springs was 0.5 m, the load-bearing area of each spring in central areas 1 and 2 was 0.25 m^2 and at the edge and corners was 0.125 m^2 and 0.0625 m^2, respectively.

3.8 Proposed equations for final displacement and final stress

The elastic displacement of foundations in different

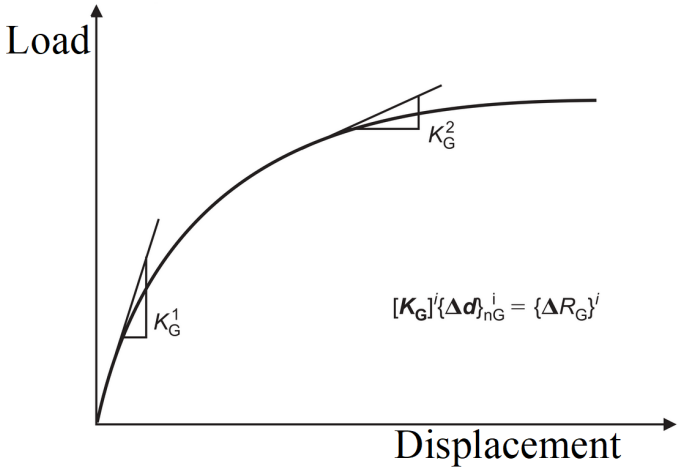

Fig. 15 Load-displacement curve (Potts 2003)

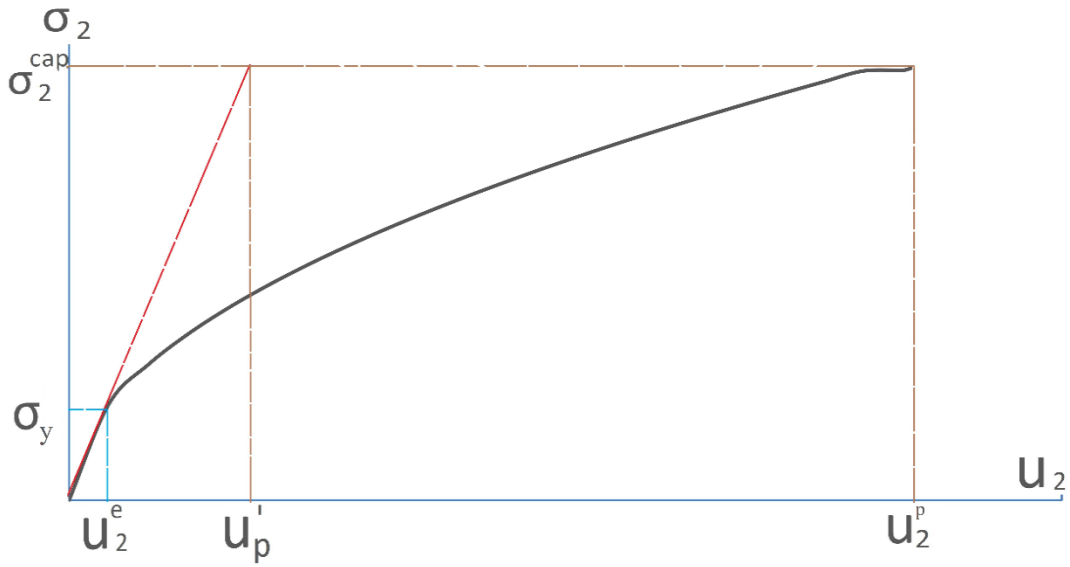

Fig. 16 Elastic, perfectly plastic stress-displacement curve

types of soil can be obtained using Eqs. (14) and (15) (Holtz 1991). C_f is a dimensionless parameter that is a function of length-to-width ratio *L/B, H* (thickness of the soil layer below the foundation) and the Poisson's ratio of the soil (μ_s). In Eq. (15), q_{avg} is equivalent to the compressive loads at the surface of the foundation. This can be obtained from the results of the loading applied to the foundation divided by the area of the foundation, and u_r is the settlement at the corner of the foundation.

$$C_f = \frac{0.85(\frac{L}{B})^{0.45}}{\left[1 + 0.1(2 + \frac{L}{B})\frac{B}{H}\right]^{1+e^{(5\mu_s^3)}}} \tag{14}$$

$$u_r = C_f \frac{q_{avg} B(1-\mu_s^2)}{E_s} \tag{15}$$

The Winkler (1867) spring method assumes that the mat foundation sits on vertical linear springs that represent deformable (linear elastic) soil. The stiffness coefficient for a Winkler spring, K_s, is called the modulus of subgrade reaction (Eq. (16)), where σ_2 is the foundation vertical pressure exerted on the soil and u_2 is the resulting vertical settlement (Loukidis 2017).

$$K_s = \frac{\sigma_2}{u_2} \tag{16}$$

In the elastic load range, the modulus of subgrade reaction is assumed to be constant (Fig. 15). However, when the soil yields, the modulus subgrade reaction decreases (Potts 2003).

In the stress-displacement curve, the slope of the curve is the modulus of subgrade reaction, which changes continuously with respect to displacement as

$$K_s = \lim_{\Delta u_2 \to 0} \frac{\Delta \sigma_2}{\Delta u_2} = \frac{d\sigma_2}{du_2} \tag{17}$$

To facilitate the back calculation stage for spring modeling, the strain stiffness after yielding can be ignored (Desai and Siriwardane 1984) and the stress-displacement

curve in the post-yield stage can be considered to be a line with zero gradients.

First, the horizontal tangent for the stress-displacement curve for maximum stress is drawn to intersect the vertical axis at the maximum stress point. By determining the elastic modulus of subgrade reaction (K_{s_e}), a line with the gradient of the elastic modulus of subgrade reaction from the origin is drawn to intersect the horizontal tangent at the point (u_p', σ_2^{cap}). This point is assumed to be the yield point of the curve (Fig. 16).

Hansen (1970) proposed the general bearing-capacity (σ_{u_H}) as

$$\sigma_{u_H} = cN_c s_c d_c + qN_q s_q d_q + 0.5B\gamma N_\gamma s_\gamma d_\gamma \quad (18)$$

And also proposed Eqs. (19)- (20)-(21)-(22) for calculating the final vertical stress and the final vertical displacement. In Eq. (19), u_p' is the vertical displacement of the foundation based on the ultimate stress and the elastic modulus of subgrade reaction at the desired point in the foundation (center, edge, or corner) as

$$u_p' = \frac{\sigma_2^{cap}}{K_{s_e}} \quad (19)$$

In Eq. (20), σ is the ratio of the ultimate stress σ_2^{cap} to the yield stress σ_y (Fig. 12)

$$\sigma = \frac{\sigma_2^{cap}}{\sigma_y} \quad (20)$$

In Eq. (21), γ_{dry}, H and E_s are the dry specific weight of soil, height of the soil profile and modulus of elasticity of the soil. The η parameter is a dimensionless parameter that is based on the final stress distribution. The factors a_1 and a_2 in Eq. (21) introduce the influence of the fiction angle (φ) on the ultimate stress (σ_2^{cap}). The results of these coefficients are shown in Table 6.

$$\begin{cases} \frac{\sigma_2^{cap}}{\sigma_{u_H}} = \eta a_1 (\frac{E_s}{\gamma_{dry} H})^{a_2} (a) \\ a_1 = 20.11\, exp(-6.76\ tan^2(\varphi)) \quad (b) \\ a_2 = 8.7\ tan^2(\varphi) + 13.7 tan^2(\varphi) - 4.676 \quad (c) \end{cases} \quad (21)$$

The final displacement u_2^p of the foundation (Fig. 12) can be calculated as

$$\frac{u_2^p}{u_p'} = -0.35\, sin(\sigma) + 0.06\sigma + 1 \quad (22)$$

As shown in Fig. 10, the stress-displacement curves are divided as a quadratic equation in terms of displacement. Dimension coefficient β is the force per cube length and coefficient α is the force per quadrat length. These two coefficients are significant for the equation of the modulus of subgrade reaction in the plastic range. The results of numerical modeling by the FE method in this research and those of Pasternak (1954), Biot (1937), Westergaard (1952), and Vesic (1961) show that the value of the modulus of subgrade reaction is a function of the area of the foundation, bending stiffness and modulus of elasticity of the soil.

In Eq. (23), u_2^e and u_2^p are the vertical elastic displacement and final vertical displacement values of the foundation as

Table 6 Parameter η in zoning area

Central 1	Central 2	Edge	Corner
1	0.835	0.5	0.35

Table 7 Parameter λ for zoning area

Central 1	Central 2	Edge	Corner
1	1.54	0.6	0.4

Table 8 Values of κ parameter in zoning area

Central 1	Central 2	Edge	Corner
1	0.94	0.475	0.3

$$\sigma_2 = g(u_2) = \begin{cases} K_{s_e} u_2 & 0 \le u_2 \le u_2^e \\ \alpha u_2 \left(u_2 + \frac{\beta}{\alpha}\right) & u_2^e < u_2 \le u_2^p \end{cases} \quad (23)$$

In Eq. (17), a derivative of vertical displacement, Eq. (24) can be obtained as

$$K_s = \begin{cases} K_{s_e} & 0 \le u_2 \le u_2^e \\ 2\alpha u_2 + \beta & u_2^e < u_2 \le u_2^p \end{cases} \quad (24)$$

To simplify, it is assumed that the modulus of subgrade reaction is constant in the range of elastic loads. The values of α and β can be obtained using Eqs. (25(a)) and (25(b)) assuming that the foundation is square. In Eqs. (25(a)) and (25(b)), A, H, h, E, I are the area of the foundation, height of the soil profile, height of the cross-section of the foundation, modulus of elasticity of the foundation and moment of inertia of the foundation, respectively. Because, in the modeled foundations, the length-to-width ratio equals one, the moment of inertia around the principal axes will be equal. Also, r_0 is the radius of the gyration of the foundation and λ and κ are dimensionless parameters based on the zoning specified in Fig. 14(c).

$$\alpha = -\frac{\lambda E_s}{10 r_0^2 \mu_s^{0.064}} \xrightarrow{L=B} \alpha = -\frac{1.2\lambda E_s}{hB\mu_s^{0.064}} \quad (25a)$$

$$\beta = \frac{\kappa \mu_s E_s A}{10 H r_0^2} \xrightarrow{L=B} \beta = \frac{1.2\kappa\mu_s B E_s}{Hh} \quad (25b)$$

Therefore, the modulus of subgrade reaction can be calculated for foundations with equal length-to-width ratios as

$$K_{s_p} = \frac{1.2\kappa B E_s \mu_s}{hH}\left(1 - \frac{2\lambda u_2}{\kappa B^2 \mu_s^{1.064}}\right) \quad (26)$$

In order to facilitate the calculation of the stress distribution and displacement in the foundations, the foundation was divided into concentric regions with a correction coefficient according to the stress-displacement results. The results of these coefficients are shown in Tables 7 and 8.

To calculate the ultimate force F_i in the spring i, Eq. (27) is used

$$F_i = \sigma_2^{cap}\ A_i \quad (27)$$

Fig. 17 shows the calculation method of the constitutive

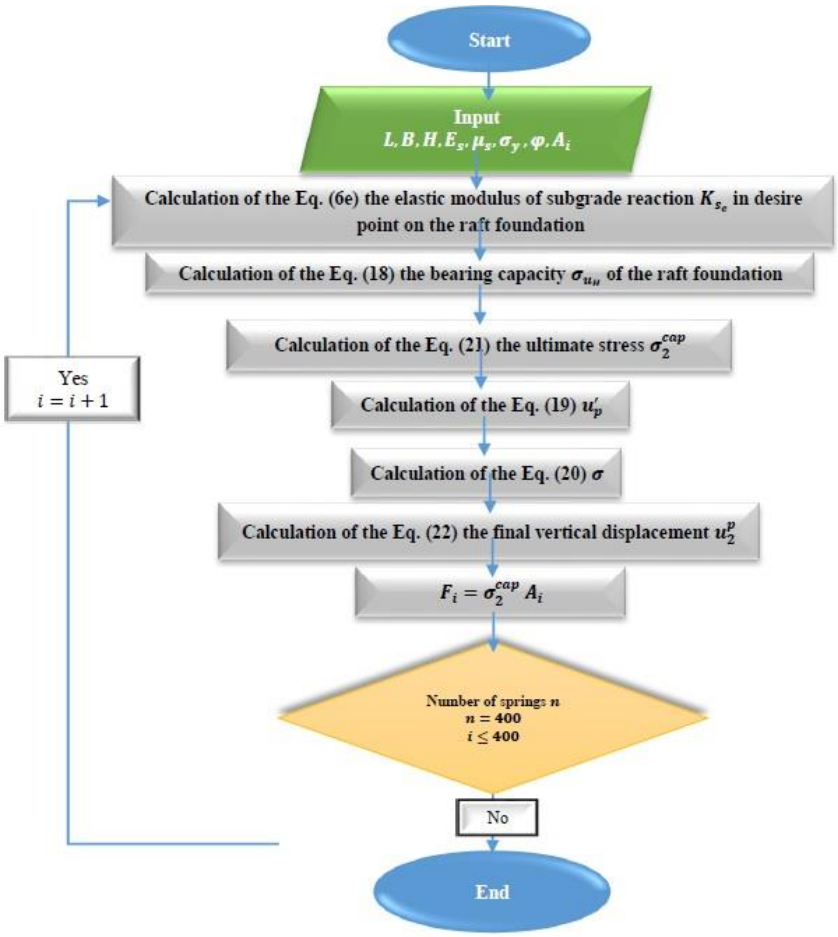

Fig. 17 Flowchart of numerical calculations of the constitutive model of springs

model for each spring at different points of the raft foundation. In this numerical modeling, based on what has been stated before, the constitutive model of the springs is elastic, perfectly plastic. Due to the accuracy of the results obtained from the FEM, this method has been used to analyse the data

4. Conclusions

Soil analysis was carried out using the finite element method with continuum 3D elements. Based on the results of cFEM, a raft foundation was placed on elastic, perfectly plastic springs. Analysis was performed to obtain the stiffness of the elastic, perfectly plastic springs and determine the distribution of the modulus of subgrade reaction for the raft foundation. The results were as follows:

- When moving from the edge to the center of the slab, the modulus of subgrade reaction decreased in the elastic range. Because the foundation was rigid, the settlement of the foundation was assumed to be similar across the slab, but the elastic vertical stress at the center of the foundation was less than at the corners and edges. In other words, in the elastic range, the stress concentration at the edges and corners increased the modulus of subgrade reaction.
- In the elastic range, an increase in the modulus of soil elasticity decreased the modulus of subgrade reaction when moving from the corner to the center of the slab. For example, at a modulus of elasticity of 123 MPa, the rate of decrease of the modulus of subgrade reaction was 33%. A decrease in the modulus of elasticity to 50 MPa reduced the modulus of subgrade reaction by 50%.
- The distribution of the modulus of subgrade reaction in the elastic range has been proposed as a six-degree symmetric polynomial in the form of a cup. This equation is a function of the layer depth, length, and width of the foundation and of the modulus of soil elasticity.
- The modulus of subgrade reaction for the half-ultimate load and ultimate load is an eight-degree polynomial. When moving from the center to the corner and edge of the foundation, the modulus of subgrade reaction increased. It was observed that, for the ultimate load, when moving from the corner to the center of the modulus of subgrade reaction at a modulus of elasticity of 123 MPa and a friction angle of 35°, the modulus of subgrade reaction increased three-fold.
- It was observed that the results of both the continuum finite element analysis and the mass-spring model were very similar, such that the vertical displacement error and vertical stress error

between the discrete spring model and continuum finite element model were 5.6% and 0.7%, respectively.

References

ABAQUS. (2016), *Analysis user's manual*, Simulia, Dassault systems. http://130.149.89.49:2080/v2016/books/usb/default.htm?startat=pt01ch03s02abx12.html.

Abdoulaye Sall, O., Fall, M., Berthaud, Y. and Makhaly, B. (2015), "Influence of mechanical properies concrete and soil on solicitaion of mat foundation", *Open J. Civil Eng.*, **5**, 249-260. http://doi.org/10.4236/ojce.2015.52025.

ACI 336.2R-88 (2002), Suggested Design Procedure for Combined Footing and Mats, American Concrete Institute; Farmington Hills, MI, USA. http://materias.fi.uba.ar/6408/Brinch%20Hansen%20%20An%20extended%20formula%20for%20bearing%20capacity.pdf.

ACI 360R-10 (2010), Guide to Design of Slabs-on-Ground, American Concrete Institute; Farmington Hills, MI, USA.

Amini, E., Golbaz, D., Amini, F., Majidi Nezhad, M., Neshat, M. and Astiaso Garcia, D.A. (2020), "Parametric study of wave energy converter layouts in real wave models", *Energies*, **13**(22), 6095. https://doi.org/10.3390/en13226095.

Amini, E., Golbaz, D., Asadi, R., Nasiri, M., Ceylan, O., Majidi Nezhad, M. and Neshat, M.A. (2021), "Comparative study of metaheuristic algorithms for wave energy converter power take-off optimisation: A case study for Eastern Australia", *J. Mar. Sci. Eng.*, **9**(5), 490. https://doi.org/10.3390/jmse905049.

Arnold, M. (1980), "Prediction of footing settlements on sand", *Ground Eng.*, **13**, 40-47.

Basile, F. (2015), "Non-linear analysis of vertically loaded piled rafts", *Comput. Geotech.*, **63**, 73-82. https://doi.org/10.1016/j.compgeo.2014.08.011.

Biot, M.A. (1937), "Bending of an infinite beam on an elastic foundation" *J. Appl. Mech. T. Am. Soc. Meeh. Eng.*, **59**, l-7. https://doi.org/10.1063/1.1712886.

Bond, D.W. (1961), "Influence of foundation size on settlement", *Geotechnique*, **11**(2), 121-143. https://doi.org/10.1680/geot.1961.11.2.121.

Bowles, J.E. (1997), *Foundation Analysis and Design*, (5th Ed), McGraw-Hill, New York, 501-519. http://thuvienso.hau.edu.vn:8888/dspace/handle/hau/4588.

Broms, B. (1964a), "Lateral resistance of piles in cohesive soils", *Soil Mech. Found. Div. - ASCE*, **90**(2), 27-63.

Desai, C.S. and Siriwardane, H.J. (1984), "Constitutive laws for engineering materials with: Emphasis on gelogic materials", *Numer. Anal. Method. Geomech.*, **8**(3), 308-309. https://doi.org/10.1002/nag.1610080310.

Dey, A., Chandra, S. and Basudhar, P.K. (2011), "Flexural response of aqueduct resting on reinforced elastic foundation subgrades", *National Conference on Recent Advances in Ground Improvement Techniques*, CBRI Roorkee, India. https://www.researchgate.net/publication/280977380.

Figueria, D., Sousa, C. and Serra Neves, A. (2018), "Winkler spring behavior in FE analyses of dowel action in statically loaded RC cracks", *Comput. Concrete*, **21**(5), 593-605. http://doi.org/10.12989/cac.2018.21.5.593.

Garg, V. and Hora, M.S. (2012), "A review on interaction behaviour of structure-foundation-soil system", *Int. J. Eng. Res.,* **2**(6), 639-644. https://citeseerx.ist.psu.edu/viewdoc/download?doi=10.1.1.640.3963&rep=rep1&type=pdf.

Hansen, J.B. (1970), "A Revised and Extended Formula for Bearing Capacity", *Danish Geotechnical Institute*, **28**, 21. http://materias.fi.uba.ar/6408/Brinch%20Hansen%20%20An%20extended%20formula%20for%20bearing%20capacity.pdf.

Hayashi, K. (1921), "Theory of Beams on Elastic Foundation", Springer-Verlag, German.

Hertz, H. (1884), "On equilibrium of floating elastic plates", *Ann. Phys. Chem.*, **22**, 449-455 (in German). https://onlinelibrary.wiley.com/doi/abs/10.1002/andp.18842580711.

Holtz, R.D. (1991), "Stress Distribution and Settlement of Shallow Foundation", *Foundation Engineering Handbook*, In: Fand H-Y, Editor, Springer, University of Washington, Washington, USA, 166-222. https://link.springer.com/chapter/10.1007%2F978-1-4615-3928-5_5.

Ismael, N.F. (1985), "Allowable pressure from loading tests on Kuwait soils", *Can. Geotech. J.*, **22**(2), 151-157. https://doi.org/10.1139/t85-021.

Ismael, N.F. (1996), "Loading tests on circular and ring plates in very dense cemented sands", *Geotech. Eng.*, **122**(4), 281-287. https://doi.org/10.1061/(ASCE)0733-9410(1996)122:4(281).

Jamil, I. and Ahmad, I. (2019), "Bending moments in raft of a piled raft system using Winkler analysis", *Geomech. Eng.*, **18**(1), 41-48. http://dx.doi.org/10.12989/gae.2019.18.1.041.

Jeong, S., Park, J., Hong, M. and Lee, J. (2017), "Variability of subgrade reaction modulus on flexible mat foundation", *Geomech. Eng.*, **13**(5), 757-774. https://doi.org/10.12989/gae.2017.13.5.757.

Kome, G.S., Ukarande, S.K., Borgaonkar, K. and Sawant, V.A. (2008), "A Parametric Study of Raft Foundation", *Proceedings of the 12th International Conference of International Assocfation for Computer Methods and Advances in Geomechanics*, Goa. India.

Lee, J., Jeong, S. and Lee, J.K. (2015), "3D analytical method for mat foundations considering coupled soil springs", *Geomech. Eng.*, **8**(6), 845-857. https://doi.org/10.12989/gae.2015.8.6.845.

Loukidis, D. and Tamiolakis, G.P. (2017), "Spatial distribution of winkler spring stiffness for rectangular raft foundation analysis", *Eng. Struct.*, **53**, 443-5. https://doi.org/10.1016/j.0engstruct.2017.10.001.

Miner, D.F. and Seastone, J.B. (1955), *Handbook of Engineering Materials*, Wiley, New York, USA.

Naeini, S.A., Ziaie Moayed, R. and Allahyari, F. (2014), "Subgrade reaction modulus (Ks) of clayey soils based on field tests", *J. Eng. Geology*, **8**(1), 2021-2046. https://www.researchgate.net/publication/286926667.

Pasternak, P.L. (1954), "On a New Method of Analysis of Elastic Foundation by Means of Two Foundation Constants", *Gosudarstvennoe Izadatelstvo Literaturi po Stroitesuvei Arkhitekture*, Russian.

Potts, D.M. (2003), "Numerical analysis: A virtual dream or practical reality", *Geotechnique*, **53**(6), 535-573. https://doi.org/10.1680/geot.53.6.535.37330.

Qin, H. and Dong Gue, W. (2014), "Limiting force profile and laterally loaded rigid piles in sand", *Appl. Mech. Mater.*, **553**, 452-457. https://doi.org/10.4028/www.scientific.net/AMM.553.452.

Rajashekhar Swamy, H.M., Krishnamoorthy, A., Prabakhara, D.L. and Bhavikatti S.S. (2011), "Evaluation of the Influence of Interface Elements for Structure – Isolated Footing – Soil Interaction Analysis", *Interact. Multiscale Mech.*, **4**(1), 65-83. https://doi.org/10.12989/imm.2011.4.1.065.

Reti, A.A. (1967), "Suggested design procedure for combined footing and mats. discussion of the report by ACI committee 436", *J. Am, Corner. Inst.*, **95**(3), 819-828.

Teli, S., Kundhani, P., Choksi, V., Sinha, P. and K.R. Lyer, K. (2020), "Analytical study on the influence of rigidity of foundation and modulus of subgrade reaction on behaviour of

raft foundation", *Adv. Comput. Method. Geomech*., **56**., 181-194. http://springer.nl.go.kr/chapter/10.1007%2F978-981-15-0890-5_16.

Terzaghi, K.V. (1955), "Evaluation of coefficient of subgrade reaction", *Geotechnique*, **5**(4), 297-326.

Vesic, A.B. (1961), "Beams on elastic subgrade and winkler's hypothesis", Proceedings of the *5th International Conference on Soil Mechanics and Foundation Engineering*, Paris, 845-50.

Westergaard, H.M. (2014), *Theory of Elasticity and Plasticity (Harvard Monographs in Applied Science)*, Harvard University Press, Harrisburg, PA, USA. ISBN 13: 9780674432055

Worku, A. (2009), "Winkler's single-parameter subgrade model from the perspective of an improved approach of continuum-based subgrade modeling", *J. EEA*., **26**, 11-22. https://www.ajol.info/index.php/zj/article/view/120801.

Winkler, E. (1867), "Ddie lehre von elasticital und festigkeit (on elasticity and fixity)", Dominicus, Prague. https://scholar.google.com/scholar_lookup?title=Die%20Lehre%20von%20Elastizit%C3%A4t%20und%20Festigkeit&author=E.%20Winkler&publication_year=1867

Ziaie Moayed, R. and Alibolandi, M. (2012), "Effect of elastic modulus varieties in depth on subgrade reaction modulus of granular soils", *Proceedings of the 2nd International Conference on Geotechnique, Construction Materials and Environment*, Kuala Lumpur. https://www.researchgate.net/publication/284730771_Effect_of_Elastic_Modulus_Varieties_in_Depth_on_Subgrade_Reaction_Modulus_of_Granular_Soils

Zimmermann, H. (1888), "Calculation of the upper surface construction of tailway tracks"*, Ernst and Korn Verlag*, Berlin, Germany. https://books.google.de/books?id=Y05BAQAAIAAJ&ots=YsIn25jrz4&dq=Zimmermann%2C%20H.%20(1888)%2C&lr&pg=PR3#v=onepage&q=Zimmermann,%20H.%20(1888),&f=false

CC